

The protein tyrosine phosphatase PTP1B is a negative regulator of CD40 and BAFF-R signaling and controls B cell autoimmunity

David Medgyesi,^{1,2,3} Elias Hobeika,^{1,2,3} Robert Biesen,⁴ Florian Kollert,⁵ Adriano Taddeo,⁶ Reinhard E. Voll,⁵ Falk Hiepe,⁴ and Michael Reth^{1,2,3}

¹BIOSS Centre for Biological Signalling Studies; and ²Department of Molecular Immunology, Institute of Biology III, Faculty of Biology; University of Freiburg, D-79104 Freiburg, Germany

³Max Planck Institute of Immunobiology and Epigenetics, D-79108 Freiburg, Germany

⁴Medical Department, Division of Rheumatology and Clinical Immunology, Charité University Medicine Berlin, D-10117 Berlin, Germany

⁵Department of Rheumatology and Clinical Immunology, University Medical Center Freiburg, D-79106 Freiburg, Germany

⁶German Rheumatism Research Centre, Leibniz Association, D-10117 Berlin, Germany

Tyrosine phosphorylation of signaling molecules that mediate B cell activation in response to various stimuli is tightly regulated by protein tyrosine phosphatases (PTPs). PTP1B is a ubiquitously expressed tyrosine phosphatase with well-characterized functions in metabolic signaling pathways. We show here that PTP1B negatively regulates CD40, B cell activating factor receptor (BAFF-R), and TLR4 signaling in B cells. Specifically, PTP1B counteracts p38 mitogen-activated protein kinase (MAPK) activation by directly dephosphorylating Tyr¹⁸² of this kinase. Mice with a B cell-specific PTP1B deficiency show increased T cell-dependent immune responses and elevated total serum IgG. Furthermore, aged animals develop systemic autoimmunity with elevated serum anti-dsDNA, spontaneous germinal centers in the spleen, and deposition of IgG immune complexes and C3 in the kidney. In a clinical setting, we observed that B cells of rheumatoid arthritis patients have significantly reduced PTP1B expression. Our data suggest that PTP1B plays an important role in the control of B cell activation and the maintenance of immunological tolerance.

CORRESPONDENCE

Michael Reth:
michael.reth@bioss.uni-freiburg.de
OR

David Medgyesi:
medgyesi@ie-freiburg.mpg.de

Abbreviations used: BCR, B cell antigen receptor; CIP, calf intestinal phosphatase; DMARD, disease-modifying antirheumatic drug; FO, follicular; MAPK, mitogen-activated protein kinase; MZ, marginal zone; PLA, proximity ligation assay; PNA, peanut agglutinin; PTP, protein tyrosine phosphatase; RA, rheumatoid arthritis; TD, T cell dependent; TI, T cell independent.

The B cell antigen receptor (BCR) mediates the antigen-specific activation of B cells, leading to their proliferation and differentiation into antibody-secreting plasma cells. In a T cell-dependent (TD) immune response, interaction with helper T cells stimulates B cells to switch to high-affinity IgG antibody production. This process is regulated by co-receptors, most importantly by the TNF receptor family member CD40 (Elgueta et al., 2009). Another member of this family, namely the B cell activating factor receptor (BAFF-R), is involved in survival signals in B cells (Gross et al., 2001; Schiemann et al., 2001). The downstream signaling of activated B cells includes several tyrosine phosphorylation steps, which are under the tight control of protein tyrosine phosphatases (PTPs; Pao et al., 2007a; Kurosaki and Hikida, 2009). Most nonreceptor PTPs play an inhibitory role in the regulation of B cell activation; therefore, they are important to maintain immunological

tolerance. Indeed, loss of PTP function can lead to autoimmune disorders (Vang et al., 2008).

PTP1B (encoded by *Ptpn1*) is a ubiquitously expressed PTP comprising an N-terminal catalytic domain, a proline-rich region, and a hydrophobic C terminus that localizes the enzyme at the cytoplasmic face of the ER (Frangioni et al., 1992). PTP1B can also be released from the ER and relocated to the cytoplasm by a calpain-mediated proteolytic cleavage (Frangioni et al., 1993). PTP1B is an important negative regulator of the insulin receptor and various growth factor receptors, such as epidermal growth factor, platelet-derived growth factor, and insulin-like growth factor-I receptors (Cicirelli et al., 1990; Lammers et al., 1993). PTP1B also limits Toll-like

© 2014 Medgyesi et al. This article is distributed under the terms of an Attribution-Noncommercial-Share Alike-No Mirror Sites license for the first six months after the publication date (see <http://www.rupress.org/terms>). After six months it is available under a Creative Commons License (Attribution-Noncommercial-Share Alike 3.0 Unported license, as described at <http://creativecommons.org/licenses/by-nc-sa/3.0/>).

receptor signaling in macrophages (Xu et al., 2008) and inhibits leptin receptor signaling by dephosphorylating the receptor-associated kinase JAK2 (Myers et al., 2001). Other nonreceptor tyrosine kinases, including c-Src, Bcr-Abl, and TYK2, as well as the transcription factor STAT6, are also substrates of PTP1B (LaMontagne et al., 1998; Bjorge et al., 2000; Myers et al., 2001; Lu et al., 2008). PTP1B-deficient mice are resistant to diet-induced obesity and are hypersensitive to insulin (Elchebly et al., 1999). Additionally, PTP1B promotes the development of breast cancer by activating c-Src in ErbB2-mediated transformation (Bentires-Alj and Neel, 2007; Julien et al., 2007; Arias-Romero et al., 2009).

It has been reported that PTP1B-deficient mice have increased numbers of pro- and pre-B cells (IgM⁻, IgD⁻) in the bone marrow and higher proportions of B cells in lymph nodes and aged mice showed lymphadenopathy (Dubé et al., 2005). However, as PTP1B is ubiquitously expressed, these effects may not be entirely B cell autonomous. To study the role of PTP1B in B cell development and in the regulation of mature B cells, we generated mice with a B cell-specific deletion of *Ptpn1*. Here, we show that PTP1B regulates CD40 and BAFF-R signaling and dephosphorylates the mitogen-activated protein kinase (MAPK) p38. Furthermore, we found that a deficiency or down regulation of PTP1B is associated with autoimmunity in mice and humans.

RESULTS

Ptpn1^{fl/fl}-mb1cre mice show no impairment of B cell development

To study B cell-specific functions of PTP1B, we crossed mice carrying floxed *Ptpn1* alleles (Bence et al., 2006) together with mb1cre mice. The latter have the mammalian codon-optimized hCre recombinase inserted into the *mb-1* locus (encoding the BCR signaling subunit Igα; Hobeika et al., 2006). In these mice, hCre is expressed exclusively in the B cell lineage from the early pro-B cell stage on. First we confirmed that the deletion of floxed *Ptpn1* alleles is restricted to B cells. We genotyped tail biopsies and different populations from the bone marrow (B220⁺-IgM⁻, B220⁺-IgM⁺, B220⁻, IgM⁻) and the spleen (CD19⁺, Thy1.2⁺). The floxed allele was efficiently deleted in B cells in the presence of the mb1cre allele, and there was no detectable deletion in the non-B cell fractions (Fig. 1 A). We then analyzed the B cell populations of different developmental stages based on defined surface marker patterns and found no major difference in *Ptpn1^{fl/fl}*-mb1cre compared with *Ptpn1^{+/+}*-mb1cre or *Ptpn1^{fl/fl}* control mice (Fig. 1, C and D). Total B cell numbers in the bone marrow and in the spleen were also similar in these animals (Fig. 1 B).

PTP1B-negative B cells respond better to anti-CD40 and BAFF stimulus

To investigate the role of PTP1B for the expansion of mature B cells, we exposed purified CD43⁻ splenic B cells to different stimuli and analyzed their proliferation by measuring [³H]thymidine incorporation. The PTP1B-deficient B cells display the same proliferative response as B cells from control

mice when cultured with anti-IgM or anti-IgM and IL-4 (Fig. 2 A). However, when stimulated with anti-CD40, the PTP1B-deficient B cells showed a significantly higher proliferation rate than control B cells (Fig. 2 A). Another important TNF family receptor on the B cell surface apart from CD40 is the BAFF-R, which regulates the survival of B cells in the periphery. We tested the survival of splenic B cells, isolated from control or *Ptpn1^{fl/fl}*-mb1cre mice, in the presence of BAFF. After 10 d of culturing, the PTP1B-deficient B cells showed a significantly higher survival rate, suggesting that PTP1B also regulates BAFF-R signaling (Fig. 2 B).

We also studied the proliferative response of the CD43⁻ splenic B cells of control and *Ptpn1^{fl/fl}*-mb1cre mice with TLR2, -3, -4, -7, and -9 stimulations. When the cells were treated with ligands for TLR2, -3, -7, and -9, we did not observe any major difference between the control and PTP1B⁻ cells (not depicted). However, PTP1B⁻ B cells proliferated significantly better than the control cells in response to LPS stimulus (Fig. 2 A).

To analyze in more detail which subpopulations of splenic B cells are affected the most in the CD40- and BAFF-R-mediated proliferation and survival responses, we repeated these experiments on sorted transitional (T1-2 and T3), marginal zone (MZ), and follicular (FO) B cells. The cells were labeled with CFSE and stimulated with anti-IgM, anti-CD40, BAFF, or anti-IgM and BAFF together and analyzed by flow cytometry after 4 d. At the time of the measurement, the cells were also labeled with 7AAD to gate on the living population. These experiments showed that mainly the FO and MZ B cells drive the elevated proliferation of PTP1B-deficient B cells upon anti-CD40 stimulation (Fig. 2, D and E). The PTP1B⁻ transitional populations and the MZ B cells showed a higher survival rate than the control cells in the presence of BAFF already after 4 d (Fig. 2 F). Interestingly, especially the PTP1B-deficient MZ B cells but also the T1-2 population showed higher survival upon anti-IgM stimulus compared with the respective control population (Fig. 2 F). PTP1B⁻ MZ B cells were also better rescued by BAFF from anti-IgM-induced cell death than the control cells (Fig. 2 F). Moreover, the surviving cells of the anti-IgM- or anti-IgM + BAFF-treated samples also showed higher proliferation than the control populations (Fig. 2 E).

We verified by flow cytometry that control and PTP1B-deficient B cells express similar amounts of CD40, BAFF-R, and TLR4 on their cell surface (Fig. 2 C and not depicted). Thus, the increased reactivity of PTP1B-deficient B cells to anti-CD40, BAFF, or LPS is not caused by increased receptor expression but rather altered signal processing.

PTP1B-deficient splenic B cells show increased p38 and Akt activation

Signal transduction from CD40 involves several pathways including the MAPK, NF-κB, and PI-3 kinase pathway (Elgueta et al., 2009). To study the role of PTP1B in CD40-mediated signaling processes, we isolated CD43⁻ splenic B cells from *Ptpn1^{fl/fl}* control and *Ptpn1^{fl/fl}*-mb1cre mice and stimulated

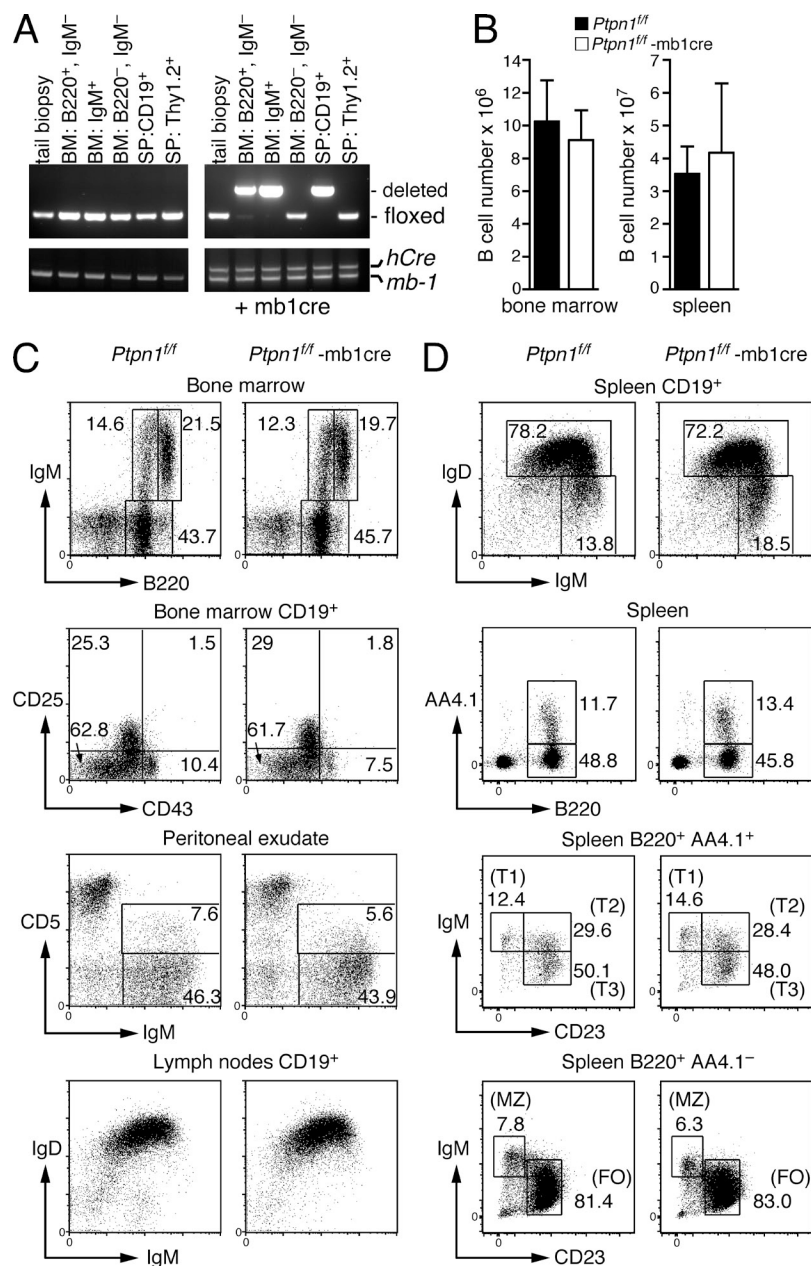


Figure 1. B cell development of *Ptpn1*^{fl/fl}-mb1cre mice. (A) Bone marrow and spleen (SP) cells were sorted by autoMACS using anti-B220, anti-IgM (for the bone marrow), anti-CD19, and anti-Thy1.2 (for the spleen). Genomic DNA was prepared, and the *Ptpn1*, *mb-1*, and *hCre* alleles were analyzed by PCR. Data shown are representative of three experiments with similar results. (B) Total B220⁺ B lineage cell numbers of bone marrow (femurs of both hind legs) and the spleen from control (*Ptpn1*^{fl/fl}) and *Ptpn1*^{fl/fl}-mb1cre mice were determined by flow cytometry. Data are shown as mean ± SD (n = 5). (C) Bone marrow, peritoneal exudate, and lymph nodes were harvested from *Ptpn1*^{fl/fl} (left) and *Ptpn1*^{fl/fl}-mb1cre (right) mice, and the expression of the indicated surface markers was assessed by flow cytometry. Numbers represent percentages inside the lymphocyte gate or the CD19⁺ gate. (D) Spleen samples from *Ptpn1*^{fl/fl} (left) and *Ptpn1*^{fl/fl}-mb1cre (right) mice. Numbers represent percentages inside the lymphocyte gate or the gate indicated at the top of each panel. Figures are representative of five experiments with similar results.

them for different times with anti-CD40. The phosphorylation and expression of signaling molecules downstream of CD40 were analyzed by Western blotting. Although the activation of the JNK and NF- κ B pathways was not affected by the PTP1B deletion, we observed higher p38 and Akt phosphorylation in PTP1B-deficient B cells (Fig. 3 A). Depending on the cell type, p38 regulates several downstream molecules (Cuadrado and Nebreda, 2010). In B cells, MK2 (MAPKAPK-2) is a key substrate of p38, playing an important role in the proliferation and class switch recombination of these cells (Craxton et al., 1998). MK2 directly phosphorylates Hsp27, a small heat shock protein which has an important role in actin rearrangement during B cell activation. In line with the p38 phosphorylation data, we found that upon

anti-CD40 stimulation, the p38 downstream targets MK2 and Hsp27 are also more strongly phosphorylated in PTP1B-deficient B cells than in the control samples (Fig. 3 A).

Because PTP1B-deficient B cells survived better in the presence of BAFF, we next analyzed the signal transduction from the BAFF-R in a 0–4-h time frame. We found increased p38 and Akt phosphorylation in PTP1B-deficient B cells in comparison with control B cells (Fig. 3 B). The activation of the alternative NF- κ B pathway, however, was unchanged in the PTP1B-deficient B cells (Fig. 3 B), even when we stimulated the cells for 12–18 h (not depicted). The response to BCR triggering with anti-IgM antibody F(ab')₂ fragments did not reveal an altered p38 or Akt phosphorylation between PTP1B-deficient or -sufficient B cells (Fig. 3 C). This finding

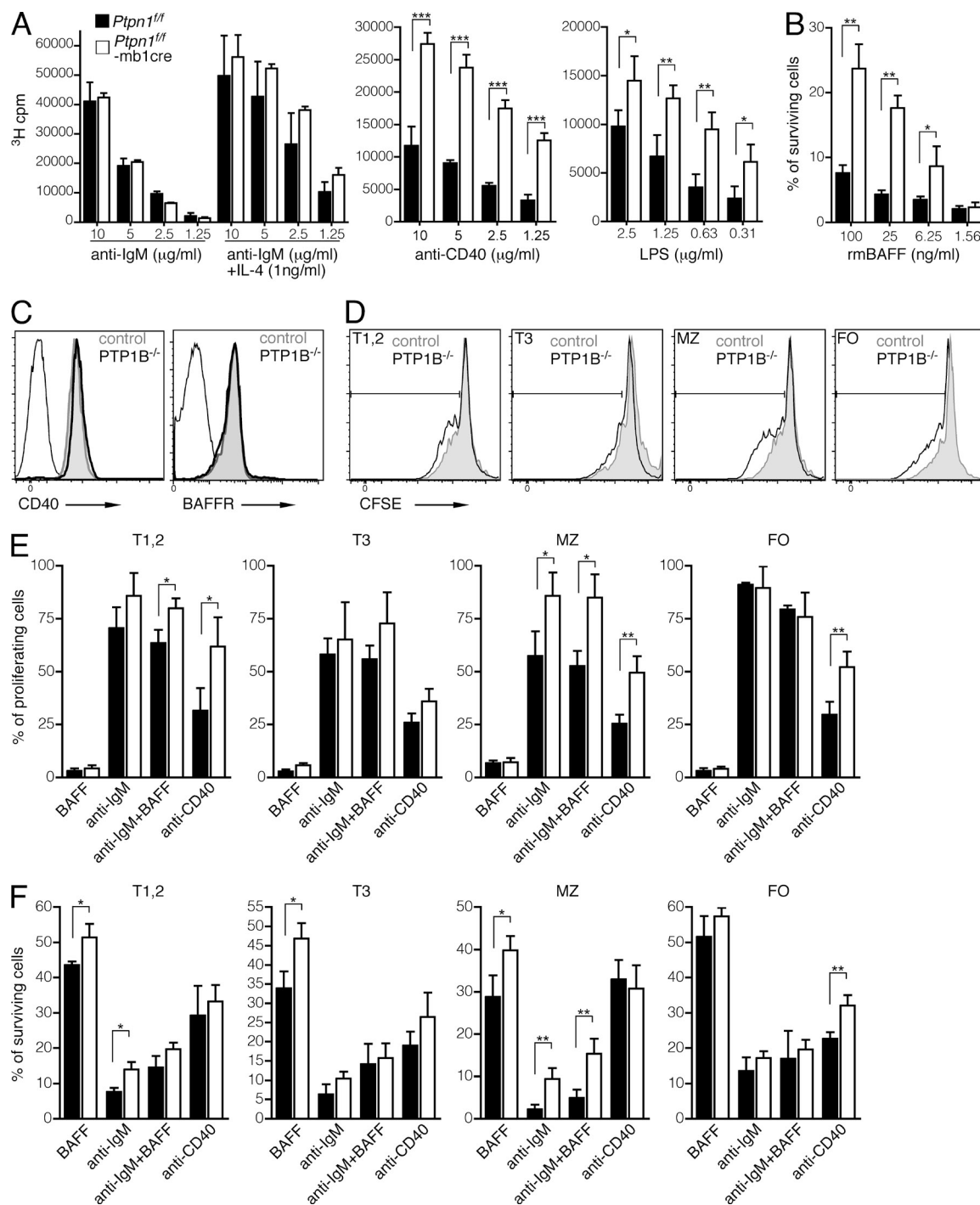


Figure 2. PTP1B-deficient B cells show increased proliferation in response to anti-CD40 and LPS and higher survival rate in response to BAFF. (A) CD43⁻ B cells from the spleen of 9–10-wk-old control (*Ptpn1^{fl/fl}*) and *Ptpn1^{fl/fl}-mb1cre* mice were cultured with anti-IgM F(ab')₂, anti-IgM F(ab')₂ + IL-4, anti-CD40, or LPS for 36 h, and then [³H]thymidine was added for an additional 12 h and [³H]thymidine incorporation was measured. Data are shown as mean ± SD of three experiments. Statistical analysis was performed using one-tailed Student's *t* test (*, *P* < 0.05; **, *P* < 0.01; ***, *P* < 0.001). (B) CD43⁻ B cells from the spleen of 9–10-wk-old control (*Ptpn1^{fl/fl}*) and *Ptpn1^{fl/fl}-mb1cre* mice were cultured for 10 d in the presence of recombinant mouse BAFF added in the given concentrations. The number of surviving cells was determined by cytofluorometry using 7AAD. Results are shown as mean ± SD. Statistical analysis was performed by a one-tailed Student's *t* test (*, *P* < 0.05; **, *P* < 0.01; *n* = 4 independent experiments). (C) Expression of CD40 and BAFF-R on splenic B cells of *Ptpn1^{fl/fl}* (shaded gray) and *Ptpn1^{fl/fl}-mb1cre* (thick black curve) mice were determined by flow cytometry (isotype control is shown as a thin black curve). Data shown are from the CD19⁺ lymphocyte gate and representative of three experiments. (D–F) Splenic B cells were sorted to T1-2, T3, MZ, and FO populations (according to the gating strategy shown in Fig. 1 D [bottom]), labeled with CFSE, and then stimulated with 25 ng/ml rmBAFF, 10 μg/ml anti-IgM F(ab')₂, 10 μg/ml anti-IgM F(ab')₂ together

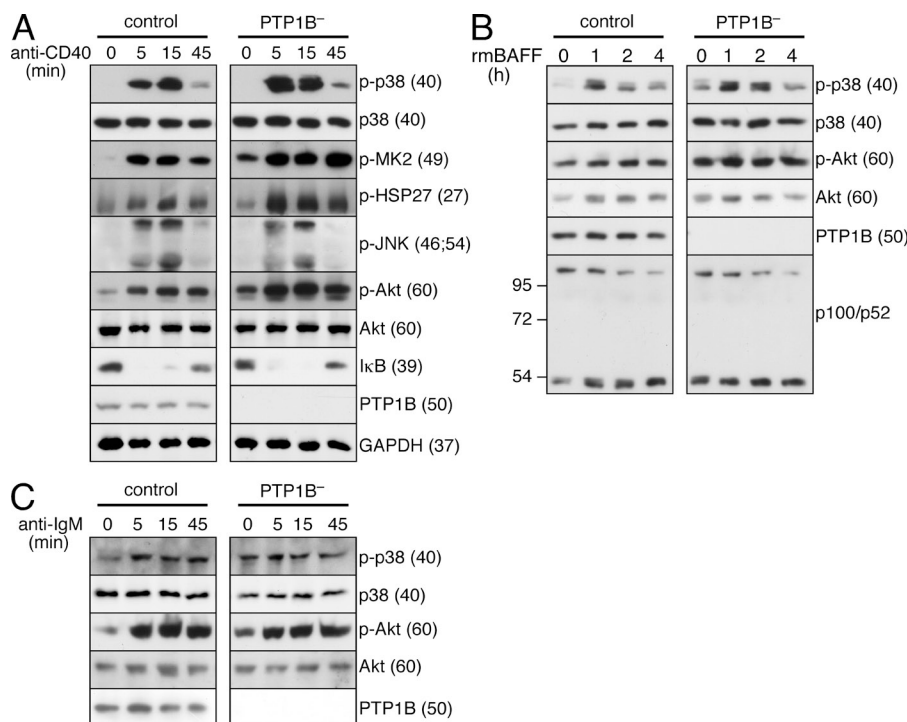


Figure 3. CD40, BAFF-R, and BCR signaling of isolated splenic B cells.

(A–C) CD43⁺ B cells from the spleen of 9–10-wk-old control (*Pttn1^{fl/fl}*) and *Pttn1^{fl/fl}-mb1cre* mice were stimulated with 10 μ g/ml anti-CD40 (A), 50 ng/ml recombinant mouse BAFF (B), or 10 μ g/ml anti-IgM F(ab')₂ (C) for the given times. The activation of the indicated downstream signaling molecules was studied by Western blot. (Phosphorylated forms of the molecules are marked as “p-.”) The data shown are representative of three experiments with similar results. The molecular masses of the bands (in kilodaltons) are indicated in parentheses.

is in agreement with the proliferation data and shows that PTP1B dominantly controls TNF family receptors rather than antigen receptor signaling. Note that the BCR stimulation induces much weaker p38 activation than CD40 triggering, as has been described previously (Craxton et al., 1998).

p38 MAPK is a direct substrate of PTP1B

Upon activation, p38 MAPK is phosphorylated on threonine and tyrosine residues. Thus, it is a potential substrate of PTPs. To test for a colocalization between p38 MAPK and PTP1B, we performed a proximity ligation assay (PLA) on fixed splenic B cells that were either left untreated or stimulated with anti-CD40 before fixation. The fixed and permeabilized cells were incubated with oligonucleotide-coupled p38- and PTP1B-specific antibodies and subjected to a PLA reaction. A fluorescent signal indicating the close proximity of p38 and PTP1B was strongly induced in B cells treated with anti-CD40 for 10 min, showing that their colocalization is triggered by the stimulus (Fig. 4, A and B). As a negative control, PTP1B-deficient splenic B cells did not give a PLA signal (Fig. 4, A and B). Using an anti-JNK together with the anti-PTP1B antibody in the PLA reaction also did not give a positive signal (Fig. 4, A and B). This finding is in line with our Western blot analysis (Fig. 3 A) and suggests that in

anti-CD40-stimulated B cells, PTP1B specifically associates with p38 but not with JNK.

To confirm the interaction of PTP1B with p38, we expressed FLAG-tagged fusion proteins containing either WT or a substrate-trapping mutant (D¹⁸¹A) of PTP1B in A20 mouse B lymphoma cells. The D¹⁸¹A mutant is catalytically inactive, but it is still able to bind and trap the substrate (Flint et al., 1997). The FLAG-tagged PTP1B was immunoprecipitated from the lysate of untreated or anti-CD40-stimulated A20 cells, and the samples were subjected to Western blotting. More p38 was coprecipitated with the D¹⁸¹A mutant PTP1B from the lysates of anti-CD40-stimulated B cells, suggesting that p38 is a direct substrate of PTP1B (Fig. 4 C).

The dual-specificity kinase MKK6 is known to phosphorylate the activation loop of p38 at T¹⁸⁰ and Y¹⁸². To test whether PTP1B interacts with the dual-phosphorylated p38, we expressed the FLAG-tagged PTP1B (WT or D¹⁸¹A) with or without a constitutively active MKK6 (ca-MKK6) in A20 B cells (Raingeaud et al., 1996). In this experiment, more p38 was coprecipitated together with WT or the D¹⁸¹A mutant of PTP1B from the lysates of cells expressing ca-MKK6 (Fig. 4 D). This shows that the phosphorylation of p38 increases its interaction with PTP1B.

To show that PTP1B not only binds but also dephosphorylates Y¹⁸² of p38, we performed an in vitro phosphatase

with 25 ng/ml rmBAFF, or 10 μ g/ml anti-CD40. After 4 d, the dead cells were stained with 7AAD, and the proliferation was measured by flow cytometry. (D) Proliferation of anti-CD40-stimulated cells. (E) Percentage of proliferating 7AAD⁺ cells (see CFSE gating in D). (F) Percentage of 7AAD⁺ cells of the total population. Results are shown as mean \pm SD. Statistical analysis was performed by a two-tailed Student's *t* test (*, *P* < 0.05; **, *P* < 0.01; *n* = 3 independent experiments).

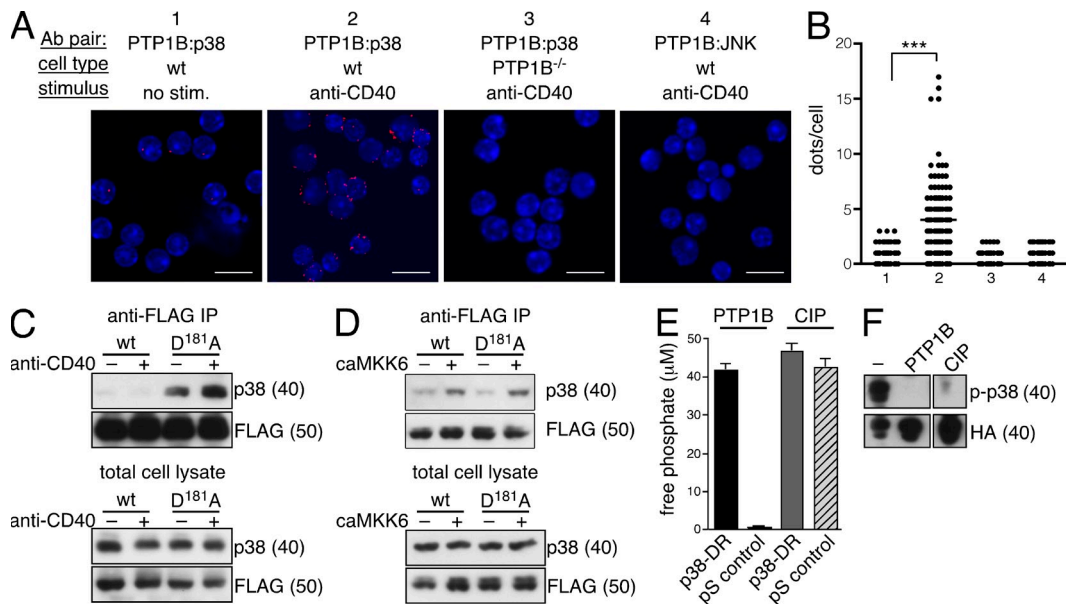


Figure 4. p38 is a substrate of PTP1B. (A) CD43⁻ B cells from the spleen of 9–10-wk-old control (*Ptpn1^{fl/fl}*) and *Ptpn1^{fl/fl}*-mb1cre mice were immobilized on glass slides and stimulated with 10 μ g/ml anti-CD40 for 10 min, and colocalization of PTP1B and p38 was visualized by confocal microscopy using the PLA method. PTP1B and JNK interaction is shown as a control. The data shown are representative of three experiments with similar results. Bars, 10 μ m. (B) Analysis of the PLA data was performed with the BlobFinder software. Each dot represents one cell. Statistical analysis was performed using a Mann-Whitney test (***, $P < 0.001$). (C and D) A20 B lymphoma cells were transfected with FLAG-tagged PTP1B WT and the D¹⁸¹A substrate trapping mutant. Cells were either stimulated by anti-CD40 (C) or cotransfected with constitutively active MKK6 (D). PTP1B was precipitated by anti-FLAG. Samples were analyzed by Western blot. Results shown are representative of three independent experiments with similar results. (E) Synthetic peptide representing amino acids 177–186 of p38 MAPK (p38-DR) was used as a substrate for PTP1B in an *in vitro* phosphatase assay. Free phosphate in the solution was measured by Malachite green. A serine-phosphorylated peptide was used as a negative control (pS control). CIP was applied as a positive control for the phosphatase activity. Results are shown as the mean \pm SD of three experiments. (F) Constitutively active MKK6 was coexpressed with HA-tagged p38 in S2 cells. Immunoprecipitated p38 (phosphorylated on T¹⁸⁰ and Y¹⁸²) was used as a substrate for PTP1B in *in vitro* phosphatase assay, and the samples were analyzed by Western blot. CIP was used as positive control. The data shown are representative of three experiments with similar results. (C, D, and F) The molecular masses of the bands (in kilodaltons) are indicated in parentheses.

assay with a synthetic phosphopeptide (DR) corresponding to the activation site of p38 (D¹⁷⁷-pY¹⁸²-R¹⁸⁶). In this assay, the phosphatase activity was measured by the release of the free phosphate. Recombinant PTP1B expressed and purified from *Escherichia coli* efficiently dephosphorylated the phosphotyrosine of the DR peptide, but not the phosphoserine of a control peptide (pS control). Calf intestinal phosphatase (CIP) was used as a positive control for phosphatase activity (Fig. 4 E).

To confirm that PTP1B can dephosphorylate the dual phosphorylated (T¹⁸⁰ and Y¹⁸²) p38, we coexpressed HA-tagged p38 and ca-MKK6 in S2 cells. The phosphorylated p38 was then immunopurified and incubated with either recombinant PTP1B or CIP (as a positive control). After SDS-PAGE and Western blotting, the membrane was probed with an anti-phospho-p38 antibody that detects only the double-phosphorylated p38 (Fig. 4 F). This assay clearly showed that dual-phosphorylated p38 is a substrate of PTP1B.

Ptpn1^{fl/fl}-mb1cre mice have an elevated TD immune response

The CD40L-CD40 interaction plays an important co-stimulatory role in the T/B cell collaboration and the establishment of a TD immune response. This co-stimulatory signal is also required for class switch recombination and affinity maturation of B cells. The T cell-independent (TI) immune

response results mainly in low-affinity IgM production and does not require CD40. We next analyzed the immune responses of PTP1B-deficient *Ptpn1^{fl/fl}*-mb1cre mice exposed to either TI (TNP-Ficoll) or TD (TNP-BSA) antigens.

Immune sera collected on day 7 after the immunization with TNP-Ficoll did not show a significant difference of antigen-specific IgM titers between *Ptpn1^{fl/fl}*-mb1cre and control mice (Fig. 5 A). To elicit a TD immune response, mice were immunized on day 0 and boosted on day 21 with TNP-BSA. Immune sera were collected on days 14, 21 (pre-boost), 28, and 35. *Ptpn1^{fl/fl}*-mb1cre mice showed elevated antigen-specific IgG levels in the primary (day 14 and 21) and secondary immune responses (day 28 and 35) compared with control littermates (Fig. 5 B). The finding of an increased TD immune response in *Ptpn1^{fl/fl}*-mb1cre mice is in line with our biochemical experiments showing an increased CD40 signaling in PTP1B-deficient B cells.

Ptpn1^{fl/fl}-mb1cre mice have elevated serum IgG and anti-dsDNA levels

The analysis of the total serum IgG titers showed that the *Ptpn1^{fl/fl}*-mb1cre mice have an elevated serum IgG concentration compared with control littermates (Fig. 6 A). The isotype-specific ELISAs showed higher concentrations of all four IgG

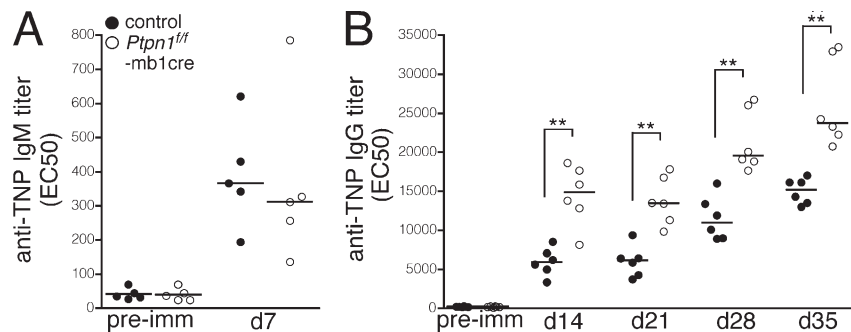


Figure 5. Immune response of *Ptpn1^{fl/fl}-mb1cre* mice. (A) 9–10-wk-old control and *Ptpn1^{fl/fl}-mb1cre* mice were immunized intraperitoneally with 20 μ g TNP-Ficoll (TI antigen), and serum samples were collected before injection and on day 7 ($n = 5$ independent experiments). (B) 9–10-wk-old control and *Ptpn1^{fl/fl}-mb1cre* mice received 20 μ g TNP-BSA (TD antigen) intraperitoneally on day 0 and 21. Serum samples were collected before immunization and on day 14, 21 (before the boost), 28, and 35. Controls in both experiments (TI and TD) include both *Ptpn1^{fl/fl}* and *mb1cre* mice. Antigen-specific serum IgM (TI) or IgG (TD) titers were determined by ELISA. Each symbol represents one animal. Horizontal lines indicate the median. Statistical analysis was performed using the Mann–Whitney test (**, $P < 0.01$; $n = 6$ independent experiments). EC50, half maximal effective dilution.

isotypes (IgG1, -2a, -2b, and -3), although only the difference in IgG2a level was statistically significant (Fig. 6 A). We also observed that 52-wk-old *Ptpn1^{fl/fl}-mb1cre* mice have elevated MZ and FO B cell numbers in the spleen in comparison with control mice (Fig. 6 B). Additionally, CD43⁻ splenic B cells treated for 4 d with LPS showed increased differentiation to CD138⁺ plasma cells (Fig. 6 C).

Increased B cell numbers and total IgG concentrations can indicate a systemic autoimmune response. We thus measured the concentration of anti-dsDNA IgG in the serum of 9–10-, 35-, and 52-wk-old control and *Ptpn1^{fl/fl}-mb1cre* mice and found that the latter animals have significantly elevated anti-dsDNA antibody concentration (Fig. 6 D). A deficiency of another PTP that is prominently expressed in hematopoietic cells, namely SHP1, is also associated with autoimmunity. Indeed, SHP1-deficient mice (“motheaten” and “viable motheaten”) show a severe lethal autoimmune phenotype (Shultz and Green, 1976; Davidson et al., 1979). The B cell-specific deletion of the *Ptpn6* gene encoding SHP1 causes autoimmunity, although not as strong as that of motheaten mice in which SHP1 is deleted in all tissues (Pao et al., 2007b). We next studied whether the loss of PTP1B can increase the severity of the autoimmune disease associated with an SHP1 deficiency. For this, we crossed the *Ptpn1^{fl/fl}* mice with *Ptpn6^{fl/fl}-mb1cre* animals. A comparison of the serum anti-dsDNA titers of 9–10-wk-old control, *Ptpn6^{fl/fl}-mb1cre*, and *Ptpn1^{fl/fl}-Ptpn6^{fl/fl}-mb1cre* mice by ELISA showed that the additional deletion of *Ptpn1^{fl/fl}* significantly increased the autoimmune reaction of the *Ptpn6^{fl/fl}-mb1cre* animals (Fig. 6 E).

To provide further evidence that a PTP1B deficiency is associated with autoimmunity, we used fixed human epithelial cells (Hep-2) to probe sera from 9–10- or 52-wk-old *Ptpn1^{fl/fl}-mb1cre* mice for the presence of autoantibodies. This assay, which is also used in human diagnosis of autoimmunity (Sack et al., 2009), clearly showed that the serum of 52-wk-old *Ptpn1^{fl/fl}-mb1cre* mice contained antinuclear antibodies (Fig. 7 A). To better characterize the autoimmunity that develops with age in *Ptpn1^{fl/fl}-mb1cre* mice, we stained cryosections of spleens with peanut agglutinin (PNA), a marker of germinal center

B cells, and B220 as a B cell marker. Spleens from 52-wk-old *Ptpn1^{fl/fl}-mb1cre* mice showed spontaneous germinal center formation, whereas control spleens were negative (Fig. 7 B). We also analyzed cryosections of kidneys of these aged animals and found IgG immune complex and C3 deposition in the samples of *Ptpn1^{fl/fl}-mb1cre* mice (Fig. 7 C).

B cells isolated from rheumatoid arthritis (RA) patients have decreased *PTPN1* mRNA expression

As the B cell-specific deletion of PTP1B caused autoimmunity in mice, we asked whether a reduced expression of PTP1B is also associated with a human autoimmune disease. We therefore analyzed *PTPN1* mRNA levels (and *HPRT1* as a reference gene) of peripheral blood B cells of RA patients and healthy donors by quantitative RT-PCR (RT-qPCR). We found significantly lower expression of *PTPN1* mRNA in the samples of RA patients compared with the healthy donors (Fig. 8 A). The non-B cell fractions in the blood of RA patients, however, did not show a significantly different *PTPN1* expression to that found in healthy donors (Fig. 8 B). This indicates that the mechanism or mechanisms causing the reduction of PTP1B expression affect specifically the B cells of RA patients.

One reason for the lower PTP1B expression could be an altered composition of B cell subpopulations in the blood of RA patients compared with the healthy donors. Using CD19 as general B cell marker and three additional surface markers, we distinguished immature (CD10⁺), naive (CD10⁻, CD27⁻, CD38⁻), and memory (CD27⁺, CD38⁻) B cells and plasma cells (CD38⁺⁺, CD27⁺⁺) according to Caraux et al. (2010) and found no significant difference in the distribution of the B cell subpopulations in the blood of healthy donors and RA patients (Fig. 8 C).

We next analyzed whether the *PTPN1* expression level was influenced by the type of medical treatment given to our collection of RA patients. For this we grouped the collected data according to the different drug treatment protocols and compared them with the nontreated RA group. None of the disease-modifying antirheumatic drugs (DMARDs)

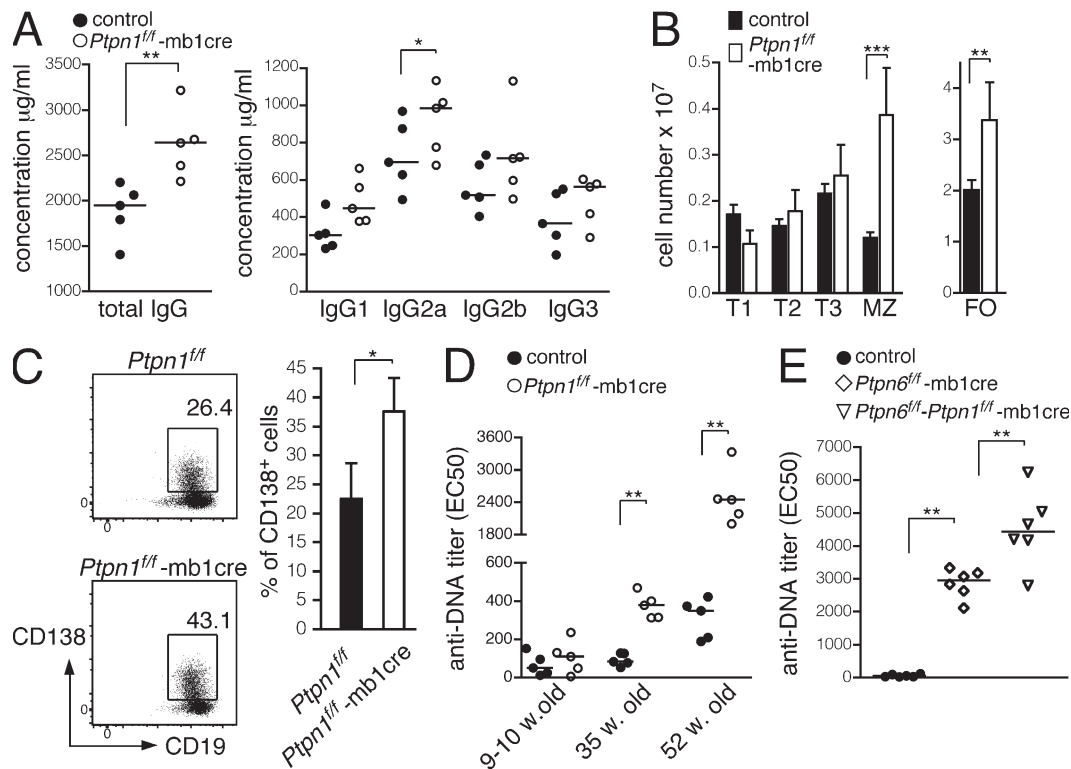


Figure 6. Serum immunoglobulin titers of *Ptpn1^{fl/fl}-mb1cre* mice. (A) Total serum IgG titers were measured in 9–10-wk-old control and *Ptpn1^{fl/fl}-mb1cre* mice. Controls include both *Ptpn1^{fl/fl}* and mb1cre mice. Each symbol represents one animal (*, $P < 0.05$; **, $P < 0.01$; $n = 5$). (B) Splenic B cell numbers of 52-wk-old control and *Ptpn1^{fl/fl}-mb1cre* mice were determined by flow cytometry (see the gating strategy in Fig. 1 D). Statistical analysis was performed by a two-tailed Student's *t* test (**, $P < 0.01$; ***, $P < 0.001$; $n = 3$). Data are shown as mean \pm SD. (C) Isolated CD43⁻ splenic B cells were cultured with 2 μ g/ml LPS. After 4 d, the cells were stained with anti-CD19 and anti-CD138 and analyzed by flow cytometry. Data shown are representative of three independent experiments. The column chart depicts the percentage of CD138⁺ plasma cells in the CD19⁺ gate as mean \pm SD. Statistical analysis was performed by a two-tailed Student's *t* test (*, $P < 0.05$; $n = 3$ independent experiments). (D) Serum anti-dsDNA titers were determined in control and *Ptpn1^{fl/fl}-mb1cre* mice of different ages. Controls include both *Ptpn1^{fl/fl}* and mb1cre mice (**, $P < 0.01$; $n = 5$). (E) Serum anti-dsDNA titers were measured in 9–10-wk-old control, *Ptpn6^{fl/fl}-mb1cre*, and *Ptpn6^{fl/fl}-Ptpn1^{fl/fl}-mb1cre* mice. Controls include both *Ptpn6^{fl/fl}* and mb1cre mice ($n = 6$). Total IgG and anti-dsDNA IgG titers were determined by ELISA. Each symbol represents one animal. Statistical analysis was performed using a Mann-Whitney test (**, $P < 0.01$). (A, D, and E) Horizontal lines indicate the median. EC50, half maximal effective dilution.

significantly affected the expression of *PTPN1*, and the same was true for the glucocorticoid treatment (Fig. 8, D and E). Most of the submitted biologicals such as CTLA4-Ig (abatacept), TNF- α blockers (etanercept and adalimumab), or anti-IL-6 (tocilizumab) also did not exert any effect on *PTPN1* expression. A remarkable exception is a group of five patients that received anti-CD20 antibodies (rituximab) 5–6 mo before the analysis. Their *PTPN1* mRNA levels were higher compared with the nontreated group (Fig. 8 F). Thus, the de novo generated B cells that develop in rituximab-treated RA patients seem to be resistant to or less affected by mechanisms that cause the low *PTPN1* levels in the RA patients. In summary, the low *PTPN1* expression in RA B cells is clearly not caused by a specific treatment protocol. We also did not find any correlation between *PTPN1* expression and age, sex, or the DAS28 (disease activity score) values of the patients (not depicted).

As mouse B cells show increased CD40 signaling in the absence of *PTPN1*, we next tested the response of the B cells

from RA patients and healthy donors to a CD40 stimulus. Isolated B cells were labeled with CFSE and cultured in the presence of CD40L + IL-4, and their proliferation was measured by flow cytometry (Fig. 8 G). This analysis shows that stimulated human B cells from RA patients proliferate faster than those from healthy donors and thus behave similarly to B cells from *Ptpn1^{fl/fl}-mb1cre* mice.

DISCUSSION

Here, we have studied *Ptpn1^{fl/fl}-mb1cre* mice with a B cell-specific deletion of *PTPN1*. Our results show that *PTPN1* is a negative regulator of CD40 and BAFF-R signaling and that the loss or reduction of *PTPN1* expression in B cells is associated with autoimmunity in mice and humans.

The *Ptpn1^{fl/fl}-mb1cre* mice have no major defect in B cell development compared with control animals. This is in contrast to a previous study on *Ptpn1^{-/-}* mice, in which a slight increase of the proportion of immature B cells in the bone marrow and of mature B cells in the peripheral lymph nodes was observed

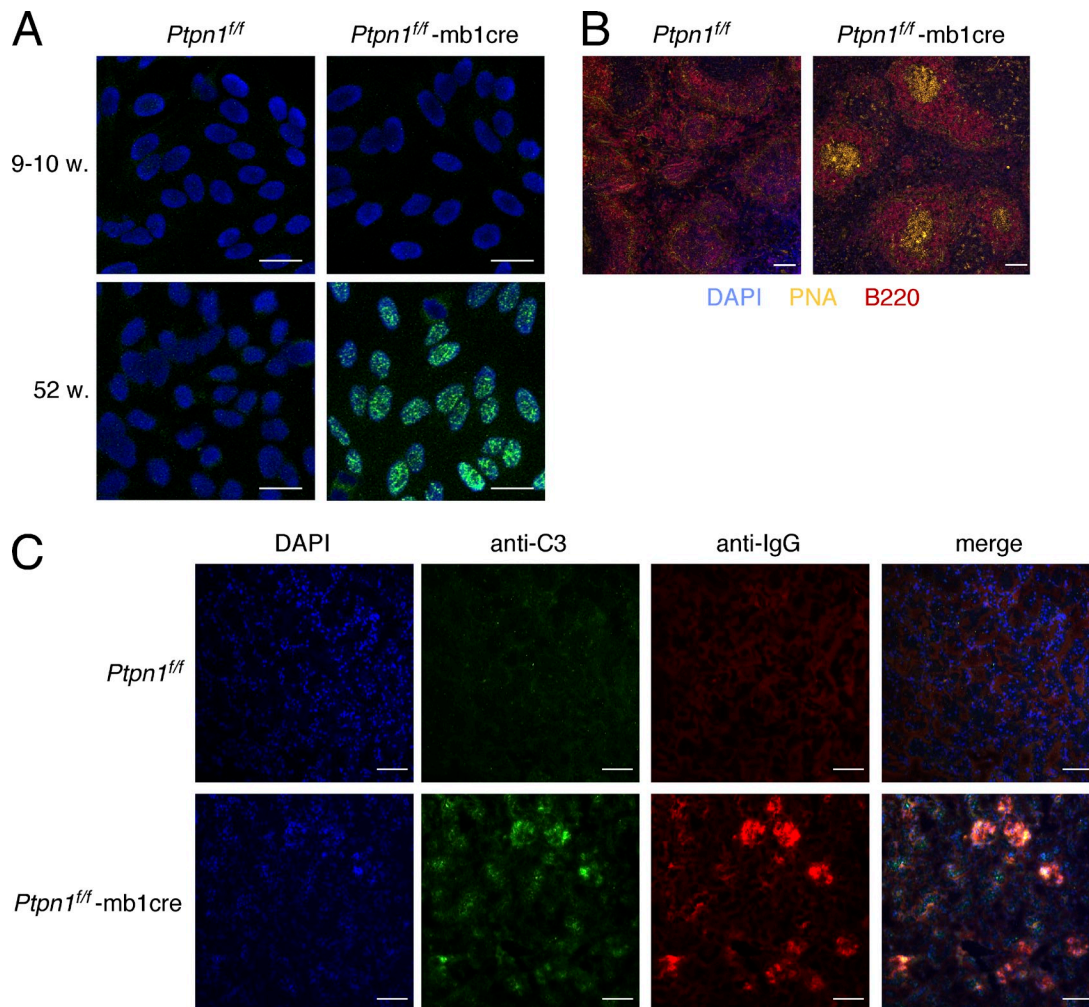


Figure 7. Aged *Ptpn1^{fl/fl}-mb1cre* mice develop autoimmunity. (A) Hep-2 slides were stained with sera from 9–10- or 52-wk-old control and *Ptpn1^{fl/fl}-mb1cre* mice and anti-IgG Alexa Fluor 488. One representative picture of each group of three mice is shown. (B) Cryosections of spleens of 52-wk-old control and *Ptpn1^{fl/fl}-mb1cre* mice were stained with PNA-biotin, streptavidin–Alexa Fluor 555 and anti-B220–Alexa Fluor 647. Nuclei were stained with DAPI. (C) Kidney cryosections from the same mice were stained with goat anti-mouse IgG–Cy3, rabbit anti-C3, and anti-rabbit Alexa Fluor 488. Nuclei were stained with DAPI. One representative picture of each group of three mice is shown. Bars: (A) 25 μ m; (B and C) 100 μ m.

(Dubé et al., 2005). Considering that the phosphatase is expressed in almost all tissues, however, the described B cell phenotype of these mice might not be B cell intrinsic.

We found that PTP1B regulates the signaling of the TNFR family members CD40 and BAFF-R. Our data also revealed that PTP1B-deficient B cells display an elevated p38 MAPK and Akt phosphorylation when stimulated via CD40 or BAFF-R. An earlier study already linked PTP1B and p38 activity and showed that a knockdown of PTP1B enhances TLR induced p38 activation in macrophages (Xu et al., 2008). However, we provide the first evidence that the dual-phosphorylated p38 MAPK is a direct substrate of PTP1B and that the two enzymes are colocalized in CD40-triggered WT B cells. The increased p38 activity in the PTP1B⁻ B cells results in an elevated phosphorylation of MK2 and HSP27 (substrates of p38), and this can explain the increased proliferation of these B cells after an anti-CD40 stimulus. Indeed, it

has been demonstrated that p38 and its substrate MK2 play a crucial role in CD40-induced proliferation of B cells. Specific inhibition of p38 strongly diminished CD40-triggered B cell proliferation (Craxton et al., 1998). This study also showed that p38 is not required for BCR-induced proliferation. The increased Akt activation in PTP1B-negative B cells could also contribute to their higher proliferation rate. It was described that inhibiting PTP1B by small molecule inhibitors resulted in elevation of Akt phosphorylation and increased proliferation of CHO/HIRc cells (Xie et al., 2003).

As indicated by the rising anti-dsDNA antibody titers, spontaneous germinal center formation in the spleen, and IgG immune complex and C3 deposition in the kidney, aged (35–52 wk old) *Ptpn1^{fl/fl}-mb1cre* mice develop autoimmunity. The elevated MZ and FO B cell compartment, the increased responsiveness of these cells to CD40, BAFF-R, and LPS, and the lower sensitivity of MZ and T1–T2 cells to BCR-induced

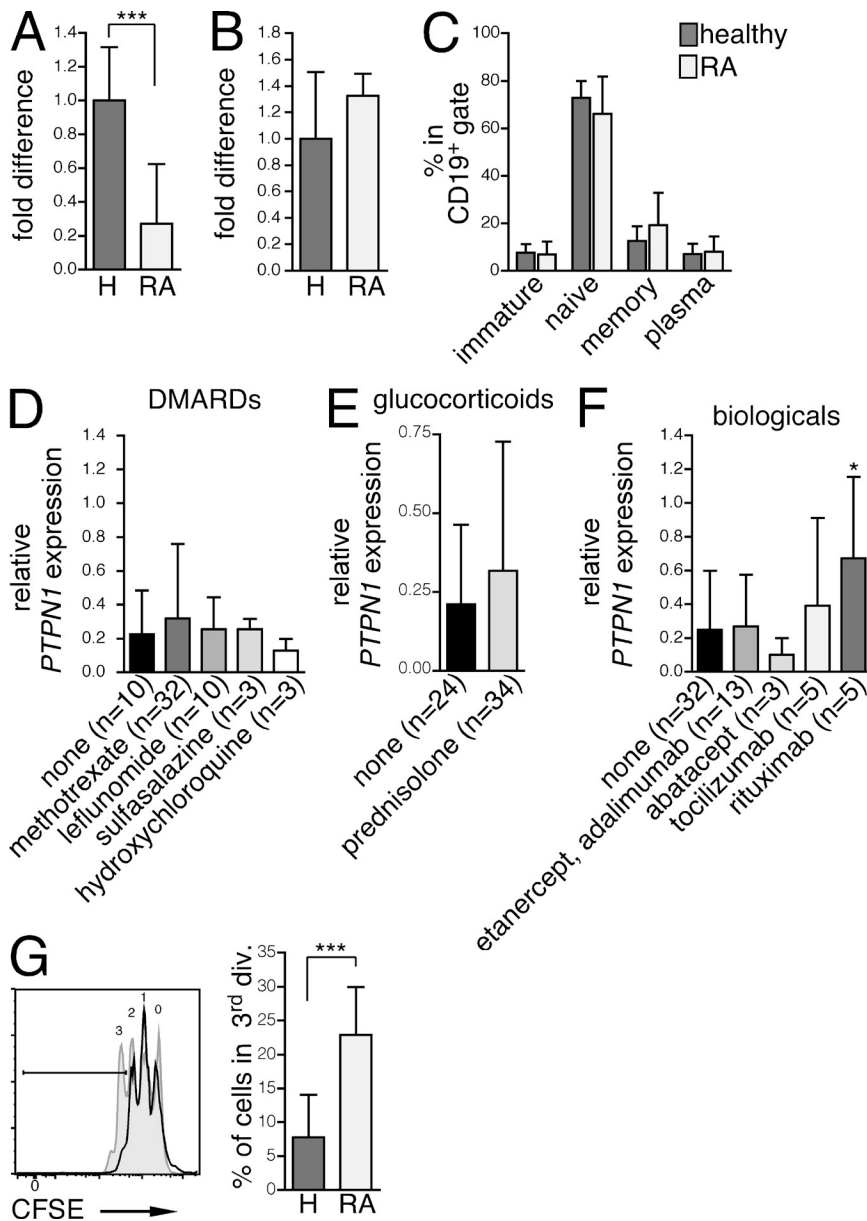


Figure 8. B cells of RA patients have decreased *PTPN1* expression. B cells from peripheral blood samples of RA patients and healthy donors were isolated, and *PTPN1* expression level was studied by RT-qPCR. (A and B) Fold difference of *PTPN1* levels from B cells (A) and non-B cells (B) of RA patients compared with the healthy donors (H: $n = 23$; RA: $n = 58$; data are shown as mean \pm SD; ***, $P < 0.001$). The abundance of mRNA was calculated by the $\Delta\Delta C_t$ method. (C) Comparison of the B cell subpopulations in RA patients and healthy donors. Isolated PBMCs were stained with CD19, CD10, CD27, and CD38 antibodies and analyzed by flow cytometry. Statistical analysis was performed with a Mann-Whitney test. (D-F) Relative *PTPN1* expression was grouped according to the medical treatments the patients received (D: DMARDs; E: glucocorticoids; F: biological agents; *, $P < 0.05$). (G) Isolated human peripheral blood B cells were labeled with CFSE and stimulated with 5 $\mu\text{g/ml}$ recombinant human sCD40L and 10 ng/ml IL-4 for 4 d. The left panel shows an example with a gate on the cells that reached the third division (healthy donor: black curve; RA patient: gray shaded curve). The bar graph depicts the percentage of the cells that reached the third division. Statistical analysis was performed by a Student's t test (***, $P < 0.001$; H: $n = 7$; RA: $n = 10$). (C-G) Data are shown as mean \pm SD.

apoptosis are likely strong contributors to autoimmunity. Despite $PTP1B^-$ B cells having elevated BAFF-R signaling, we did not observe increased MZ B cell numbers in young mice. This is in contrast to the BAFF transgenic mice that had a two- to fourfold increase in MZ B cell numbers (Mackay et al., 1999). The physiological serum BAFF concentration of WT mice is ~ 1 –5 ng/ml (Mecklenbräuer et al., 2004; Zheng et al., 2005; Matsushita et al., 2007), whereas in the BAFF Tg mice it is ~ 300 ng/ml (Batten et al., 2004). In our in vitro experiments, the markedly higher survival of $PTP1B^-$ deficient cells was at high BAFF concentrations, whereas at the range of the physiological concentrations the difference was modest or disappeared. Most likely the low physiological BAFF concentration is not sufficient to cause a higher expansion of the MZ B cell pool in young $Ptpn1^{f/f}$ -mb1cre mice.

In old mice, however, together with other factors (e.g., elevated TLR4 signals and resistance to BCR induced apoptosis), the increased BAFF-R signaling might be responsible for the higher MZ B cell numbers.

Several studies showed that TLRs (especially TLR7 and -9) play an important role in supporting the activation of autoreactive B cells (Viglianti et al., 2003; Christensen et al., 2005; Lau et al., 2005). $PTP1B^-$ deficient B cells are hypersensitive to TLR4 signals but not to TLR2, -3, -7, and -9 stimuli. The elevated TLR4 signaling in $PTP1B^-$ B cells is in accordance with earlier studies showing that $PTP1B$ is a negative regulator of LPS signaling in macrophages and that the $Ptpn1^{-/-}$ mice are more sensitive to LPS in vivo (Heinonen et al., 2006; Xu et al., 2008). Both proliferation and plasma cell differentiation of $PTP1B^-$ deficient B cells are augmented in response

to LPS, suggesting that autoreactive B cells in the periphery of *Ptpn1^{f/f}-mb1cre* mice might have a lower threshold to differentiate into autoimmune plasma cells.

The late onset of the disease is in contrast to *Ptpn6^{f/f}-mb1cre* mice with a B cell-specific deletion of SHP1, which show high-serum anti-dsDNA concentrations already at the young age of 9–10 wk. The two phosphatases thus seem to control autoimmunity in different ways. This is in line with our signaling experiments showing that PTP1B does not regulate BCR signaling, whereas SHP1 is one of the most important inhibitors of the BCR. The notion that the two phosphatases control different signaling pathways is also supported by our study of *Ptpn6^{f/f}-Ptpn1^{f/f}-mb1cre* mice with a B cell-specific deletion of PTP1B and SHP1 showing an aggravated autoimmunity in comparison with the B cell-specific SHP1 deletion alone.

We found that the mature B cells of most RA patients show a relatively modest but statistically significant decrease in *PTPN1* mRNA expression in comparison with healthy donors. These data are in line with a recent appreciation that B cells themselves, and not only the antibodies they produce, seem to play an important role in the development or maintenance of RA (Yanaba et al., 2008; Engel et al., 2011). In particular, the success of rituximab as a suitable treatment for RA supports the notion that deregulated mature B cells are involved in the disease process. We also observed that from all anti-RA treatments, those patients who received rituximab 5–6 mo before the study had a *PTPN1* expression level close to normal. It is thus feasible that B cells with low PTP1B expression, and thus probably higher p38 MAPK activity, cause or support the increased inflammation associated with RA.

An alternative explanation for the low PTP1B expression in RA B cells could be an alteration in the B cell compartments in the blood of these patients with different *PTPN1* expression levels in different B cell subtypes. Indeed, one group reported that, compared with healthy donors, RA patients have increased numbers of plasmablasts in the blood (Szyszkowski et al., 2011). In contrast, three other studies show that there is no such difference (Lin et al., 2009; Catalán et al., 2010; Mei et al., 2010). We compared the composition of the B cell pool in the blood of RA patients and healthy donors and did not find a significant difference.

What causes the low *PTPN1* mRNA expression in RA B cells is not clear. We observed that peripheral blood B cells from healthy donors stimulated by a plant mitogen phytohemagglutinin have reduced *PTPN1* mRNA expression (unpublished data). Thus, a condition with systemic inflammation causing constant activation of B cells could induce the downregulation of PTP1B. It was described that PTP1B transcription is negatively regulated by the early growth response factor 1 (Egr-1; Fukada and Tonks, 2001) and that B cell activation increases Egr-1 expression (Seyfert et al., 1990). As a consequence, high levels of Egr-1 may result in decreased PTP1B levels. However, we checked Egr-1 expression in RA B cell samples by qPCR and did not find a significant alteration (unpublished data). Thus, the regulatory mechanism causing *PTPN1* mRNA reduction needs further investigation. The

low PTP1B expression might simply be a result of RA rather than a supporting factor for the development of the disease. However, our data from the *Ptpn1^{f/f}-mb1cre* mice clearly show that the absence of PTP1B in B cells can cause autoimmunity. Therefore, we speculate that inflammatory conditions associated with RA result in low PTP1B expression and that this contributes to the disease development or progression.

Recent studies have highlighted the regulatory role of PTP1B in metabolic diseases and suggested that a specific inhibition of this phosphatase could be a promising treatment of obesity and type II diabetes. Some specific inhibitors have already entered clinical trials (Liu, 2004; Shrestha et al., 2007). According to our findings, however, such a treatment could increase the risk of autoimmune diseases and thus should be carefully monitored in this respect.

MATERIALS AND METHODS

Mice and cells. The floxed *Ptpn1* and *Ptpn6* and the *mb1cre* mice have been described previously (Bence et al., 2006; Hobeika et al., 2006; Pao et al., 2007b). *Ptpn1^{f/f}-mb1cre* animals were on a mixed FVB × BALB/c background. Control animals were littermates having the same mixed background with a genotype of either *Ptpn1^{f/f}* or *mb1cre*. The *Ptpn6^{f/f}-mb1cre* mice were on C57BL/6j and *Ptpn1^{f/f}-Ptpn6^{f/f}-mb1cre* mice were on a mixed FVB × C57BL/6j background. Genotyping was performed as described previously (Bence et al., 2006; Hobeika et al., 2006; Pao et al., 2007b). Animal experiments were carried out in compliance with guidelines of the German law. The animal experiment protocols were approved by the ethics committee of the Max Planck Institute of Immunobiology and Epigenetics (Freiburg, Germany) and the German Government authorities (Regierungspräsidium Freiburg).

B cells were isolated from the spleen of control (*Ptpn1^{f/f}*) and *Ptpn1^{f/f}-mb1cre* mice by depletion using anti-CD43 antibody-coupled magnetic microbeads (Miltenyi Biotec) and an automated magnetic cell sorter (autoMACS; Miltenyi Biotec). The negative fraction obtained by magnetic sorting was 97–98% pure B cells according to FACS analysis after staining with anti-CD19 (eBioscience) and anti-CD3 (BD). Cells were cultured in Iscove's medium (Biochrom) containing 10% heat-inactivated FCS (PAN Biotech GmbH), 2 mM L-glutamine, 100 U/ml penicillin, 100 U/ml streptomycin (Invitrogen), and 50 μM 2-mercaptoethanol (EMD). A20 mouse B lymphoma cells were cultured in RPMI 1640 medium (Gibco) containing 5% heat-inactivated FCS (PAA), 2 mM L-glutamine, 100 U/ml penicillin, 100 U/ml streptomycin, and 50 μM 2-mercaptoethanol.

Plasmid constructs and transfection. cDNA encoding PTP1B WT and the D¹⁸¹A mutant was obtained by restriction digest from the pWZL-PTP1B and pWZL-PTP1B D¹⁸¹A plasmids (LaMontagne et al., 1998; provided by M. Bentires-Alj, Friedrich Miescher Institute for Biomedical Research, Basel, Switzerland) and inserted together with a synthetic oligonucleotide, coding the FLAG-tag, to the pMIG bicistronic retroviral vector (provided by W.S. Pear, University of Pennsylvania, Philadelphia, PA) between the BglII and EcoRI sites of the MCS to construct a fusion protein with an N-terminal FLAG tag.

HA-tagged p38 was cloned into pRmHa-3 vector (Bunch et al., 1988) from pSRa-HA-p38 (gift from M. Karin, University of California, San Diego, La Jolla, CA) between the XhoI and BamHI sites of the MCS by restriction digest. Constitutively active MKK6 was cloned into the pRmHa-3 vector from pCDNA3-Flag MKK6(glu) (Addgene #13518; provided by R. Davis, Howard Hughes Medical Institute, Worcester, MA) between the SmaI and XbaI sites of the MCS by restriction digest. For cotransfection with PTP1B into A20 cells, MKK6(glu) was recloned without the FLAG tag into the bicistronic pMITHy vector (gift of S. Herzog, BIOS Centre for Biological Signalling Studies, Freiburg, Germany) by PCR-based cloning between the BglII and XhoI sites.

Transfection of S2 cells was previously described (Rolli et al., 2002). Phoenix retroviral packaging cells were transfected according to the manufacturer's

instructions using GeneJuice (EMD Millipore). Retroviral supernatants were harvested after 24 and 48 h. Viral supernatant was then added to A20 B lymphoma cells and centrifuged at 300 g at 37 °C for 3 h. GFP-positive cells were sorted by a MoFlo cell sorter (Beckman Coulter).

Flow cytometry. Cells were resuspended in PBS, 1% FCS, and 0.01% Na₂S₂O₈ and were incubated on ice with the different fluorescent-labeled antibodies. The measurement was performed with an LSR II flow cytometer (BD). All antibodies used for surface labeling were purchased from eBioscience.

Proliferation and survival assay. CD43-negative isolated splenic B cells were cultured with different stimuli at 2×10^5 cells per well in 96-well plates. After 36 h, cells were pulsed with 1 μ Ci [methyl-³H] thymidine per well for an additional 12 h, and incorporation was quantified using a Berthold-Inotech Trace-96 (Berthold) β -counter. For stimulation, F(ab')₂ anti-IgM (Jackson ImmunoResearch Laboratories, Inc.), anti-CD40 (FGK45 provided by A. Rolink, University of Basel, Basel, Switzerland), recombinant IL-4 (eBioscience), and S-form LPS (Enzo Life Sciences) were used.

For measuring the proliferation of human B cells and the different splenic B cell subpopulations of the mice, 2×10^5 cells were labeled with 1 or 3 μ g/ml CFSE (Sigma-Aldrich), respectively. The cells were then cultured in the presence of the different stimulators. For the human B cells, 5 μ g/ml recombinant human sCD40L (ImmunoTools) and 10 ng/ml IL-4 (ImmunoTools and ORF Genetics) were used. The activators for the mouse B cells are described above. After 96 h, proliferating cells were measured by flow cytometry. Dead cells were labeled with 7AAD (Enzo Life Sciences).

For the survival assay, the cells were cultured in the presence of recombinant mouse BAFF (R&D Systems) for 10 d. The dead cells were labeled with 7AAD, and the samples were measured by flow cytometry.

Cell stimulation and Western blot. Isolated splenic B cells from control (*Ptprn*^{f/f}) and *Ptprn*^{f/f}-mb1cre mice were incubated at 37°C for 5 h in Iscove's medium containing 1% FCS and then stimulated with 10 μ g/ml anti-CD40 (FGK45 provided by A. Rolink), 50 ng/ml recombinant mouse BAFF, or 10 μ g/ml F(ab')₂ anti-IgM at 37°C for different durations. Cells were then resuspended in ice-cold lysis buffer containing 50 mM Tris-HCl, pH 8, 1% Triton X-100, 137.5 mM NaCl, 1 mM EDTA, pH 8, 1 mM sodium orthovanadate, 1 mM NaF, and protease inhibitor cocktail (Sigma-Aldrich). Lysates were separated on 10% SDS-polyacrylamide gels and transferred to Hybond nitrocellulose membranes (GE Healthcare). Immunoreactive proteins were detected using a chemiluminescence detection system (ECL; GE Healthcare). Antibodies used were anti-PTP1B (EMD Millipore), anti-p-Akt, p-p38 MAPK, p-JNK, p-MAPKAPK2, p-HSP27, Akt, p38 MAPK, JNK, I κ B (Cell Signaling Technology), anti-p100/p52 (Santa Cruz Biotechnology, Inc.), and anti-GAPDH (Abcam).

Duolink and in situ PLA. Isolated splenic B cells were adhered on PTFE-coated slides (Menzel-Gläser) in Iscove's medium containing 1% FCS and then stimulated for 15 min with anti-CD40. The cells were then fixed with 2% PFA for 30 min on ice, permeabilized with 0.5% saponin for 10 min, and stained according to the manufacturer's instructions with the Duolink kit (Olink Bioscience). The antibody combinations used were rabbit anti-p38/mouse anti-PTP1B (Cell Signaling Technology and BD, respectively) or rabbit anti-JNK/mouse anti-PTP1B (Cell Signaling Technology and BD, respectively). The nuclei were stained with 1 μ g/ml Hoechst 33258. The images of the cells were taken with a confocal microscope (LSM780; Carl Zeiss; objective: 63 \times /1.4 oil immersion) and acquired with one z plane. The images were acquired with the ZEN 2010 software (Carl Zeiss), and analysis was performed using the BlobFinder software.

In vitro phosphatase assay. 15 μ g tyrosine phosphorylated synthetic oligopeptide DEMTGpYVATR (GL Biochem) corresponding to amino acids 177–186 of (mouse and human) p38 MAPK was coincubated with 0.5 μ g recombinant human PTP1B (Cayman Chemical) for 30 min at 30°C in phosphatase buffer containing 20 mM HEPES, pH 7.2, 50 mM NaCl, 5 mM

MgCl₂, and 5 mM MnCl₂. As a negative control, the serine phosphorylated CSMYEDIpSRGLQG (Eurogentec) peptide was used. As a positive control for phosphatase activity, we added 1 U CIP to the peptides in parallel samples. Free phosphate concentration was determined using the Malachite green phosphate assay kit (BioAssay Systems) according to the manufacturer's instructions. HA-tagged p38 was coexpressed with constitutively active MKK6 in S2 Schneider cells. Phosphorylated p38 was then immunoprecipitated with anti-HA antibody (Roche). The precipitated p38 was subjected to in vitro phosphatase treatment as described above. The samples were analyzed by Western blot.

Immunization. Control (*Ptprn*^{f/f} and mb1cre) and *Ptprn*^{f/f}-mb1cre mice were immunized with 20 μ g thymus-independent antigen TNP-Ficoll (Biosearch Technologies) intraperitoneally. Mice were bled before and 7 d after immunization. To determine the thymus-dependent response, control (*Ptprn*^{f/f} or mb1cre) and *Ptprn*^{f/f}-mb1cre were immunized with 20 μ g TNP-BSA (Biosearch Technologies) precipitated with alum as adjuvant and injected intraperitoneally. At day 21, a second immunization (boost) was performed with 20 μ g TNP-BSA. Mice were bled before immunization and on day 14, 21 (before the boost), 28, and 35 after injection.

ELISA. To determine antigen-specific IgM or IgG titers, 20 μ g/ml TNP-OVA (Biosearch Technologies) was used for coating (4°C overnight). For measurement of total serum IgG concentrations, 1 μ g/ml isotype-specific coating antibodies was used (IgG, IgG1, IgG2a, IgG2b, and IgG3; SouthernBiotech). The coating was performed at 4°C overnight. For the anti-dsDNA ELISA, the plates were coated with 5 μ g/ml double-stranded calf thymus genomic DNA (Sigma-Aldrich) for 2 h at room temperature. For detection, 1 μ g/ml goat anti-mouse IgM-HRPO (SouthernBiotech) or goat anti-mouse IgG-HRPO (Thermo Fisher Scientific) and as a substrate TMB (Enzo Life Sciences) were used.

Immunohistochemistry. The spleens and kidneys from 52-wk-old control (*Ptprn*^{f/f} and mb1cre) and *Ptprn*^{f/f}-mb1cre mice were frozen in Cryoblock (Mediate). (Spleens were fixed before with 4% paraformaldehyde and incubated overnight at 4°C in 30% sucrose in PBS.) 8- μ m sections were placed on glass slides, and spleen samples were stained with PNA-biotin followed by streptavidin-Alexa Fluor 555 (Invitrogen) and B220-Alexa Fluor 647 (BioLegend), whereas kidney sections were stained with anti-mouse IgG-Cy3 (Invitrogen), rabbit anti-C3 (Santa Cruz Biotechnology, Inc.), and donkey anti-rabbit Alexa Fluor 488 (BioLegend). Nuclei were stained with DAPI, and the slides were analyzed on an LSM780 confocal microscope (objective: 20 \times /0.8). Images were acquired by the ZEN 2010 software.

Study participants. RA patients ($n = 58$) were classified according to the criteria of the American College of Rheumatology/European League against Rheumatism collaborative initiative (Aletaha et al., 2010). The patient cohort included 13 males and 45 females with a mean age of 57 (range from 26 to 82) yr. Patients had a mean disease activity score 28 (DAS28) of 3.7 (range 0.84–7.16), whereof 17 were in clinical remission (DAS28 \leq 2.6), 10 had inactive (2.6 < DAS28 \leq 3.2), 19 moderate (3.2 < DAS28 \leq 5.1), and 12 active disease (DAS28 > 5.1). Erythrocyte sedimentation rate (ESR) presented with a mean of 26.9 (range 2–110) mm/h. Positive rheumatoid factor (RF) and anti-CCP antibodies (ACPAs) were detected in 41 patients; 17 patients exhibited neither RF nor ACPAs. 34 patients received glucocorticoids in a prednisolone equivalent dosage from 2 to 20 mg per day. The majority of patients were treated with DMARDs, including methotrexate ($n = 32$), leflunomide ($n = 10$), hydroxychloroquine ($n = 3$), and sulfasalazine ($n = 3$). 26 patients received biological agents: TNF- α inhibitors (etanercept or adalimumab [$n = 13$]), rituximab ($n = 5$; several months before sample collection), tocilizumab ($n = 5$), and abatacept ($n = 3$). 38 patients got nonsteroidal anti-inflammatory drugs or cox-2 inhibitors.

The group of normal donors included 19 female and 4 male individuals at the age of 29–77 yr fulfilling three criteria: (1) no history of rheumatic disease, (2) no medication, and (3) ESR < 20mm/h. The experiments applying

human material were approved by the ethical committees of the Charité University Medicine Berlin (Ethikkommission der Charité-Universitätsmedizin Berlin) and the Albert-Ludwigs-University Freiburg (Ethik-Kommission der Albert-Ludwigs-Universität Freiburg). Written informed consent was obtained from all patients and healthy donors.

Separation of B cells of RA patients. 10–15-ml blood samples were drawn into heparinized tubes and processed on Ficoll gradients (PAA Laboratories GmbH). PBMCs were recovered, and B cells were positively selected by autoMACS using anti-CD19 microbeads according to the manufacturer's instructions.

RNA isolation, RT, and real-time PCR. DNA-free RNA was extracted using the Quick-RNA MiniPrep kit (Zymo Research). Prepared RNA was reverse transcribed into cDNA using SCRIPT reverse transcriptase (Jena Bioscience) and 20 mer oligo (dT) primer. Real-time PCR reaction for *PTPN1* and *HPRT1* (as a reference gene) was performed using TaqMan Gene Expression Assays (Applied Biosystems) specific for the given genes on a 7500 Fast real-time PCR (Applied Biosystems) instrument. The relative mRNA levels were determined by the $\Delta\Delta C_T$ method.

Statistical analysis. Statistical analysis was performed by Prism 4 (GraphPad Software) and Stata software (StataCorp). The applied tests are indicated in the figure legends.

We thank Benjamin J. Neel (Ontario Cancer Institute, Toronto, Ontario, Canada) and Klaus Rajewsky (Max Delbrück Center for Molecular Medicine, Berlin, Germany) for providing the *Ptpn1* and *Ptpn6* floxed mice, as well as Mohamed Bentires-Alj and Antonius Rolink for the PTP1B plasmids and the FGK45 antibody, respectively. We are grateful to Julia Rennert, Simona Infantino, Sebastian Herzog, and Laura Kramps for technical assistance and discussions and to Peter Nielsen for critical reading of the manuscript. We thank Marton Medgyesi for his help in the statistical analysis.

This work was supported by the Deutsche Forschungsgemeinschaft through SFB746 and the Excellence Initiative of the German Federal and State Governments (EXC294). D. Medgyesi was supported by the Marie Curie Intra-European Fellowship (MEIF-CT-2006-041445).

The authors declare no competing financial interests.

Submitted: 6 June 2013

Accepted: 11 February 2014

REFERENCES

- Aletaha, D., T. Neogi, A.J. Silman, J. Funovits, D.T. Felson, C.O. Bingham III, N.S. Birnbaum, G.R. Burmester, V.P. Bykerk, M.D. Cohen, et al. 2010. 2010 rheumatoid arthritis classification criteria: An American College of Rheumatology/European League Against Rheumatism collaborative initiative. *Ann. Rheum. Dis.* 69:1580–1588. <http://dx.doi.org/10.1136/ard.2010.138461>
- Arias-Romero, L.E., S. Saha, O. Villamar-Cruz, S.-C. Yip, S.P. Ethier, Z.-Y. Zhang, and J. Chernoff. 2009. Activation of Src by protein tyrosine phosphatase 1B is required for ErbB2 transformation of human breast epithelial cells. *Cancer Res.* 69:4582–4588. <http://dx.doi.org/10.1158/0008-5472.CAN-08-4001>
- Batten, M., C. Fletcher, L.G. Ng, J. Groom, J. Wheway, Y. Laäbi, X. Xin, P. Schneider, J. Tschopp, C.R. Mackay, and F. Mackay. 2004. TNF deficiency fails to protect BAFF transgenic mice against autoimmunity and reveals a predisposition to B cell lymphoma. *J. Immunol.* 172:812–822.
- Bence, K.K., M. Delibegovic, B. Xue, C.Z. Gorgun, G.S. Hotamisligil, B.G. Neel, and B.B. Kahn. 2006. Neuronal PTP1B regulates body weight, adiposity and leptin action. *Nat. Med.* 12:917–924. <http://dx.doi.org/10.1038/nm1435>
- Bentires-Alj, M., and B.G. Neel. 2007. Protein-tyrosine phosphatase 1B is required for HER2/Neu-induced breast cancer. *Cancer Res.* 67:2420–2424. <http://dx.doi.org/10.1158/0008-5472.CAN-06-4610>
- Bjorge, J.D., A. Pang, and D.J. Fujita. 2000. Identification of protein-tyrosine phosphatase 1B as the major tyrosine phosphatase activity capable of dephosphorylating and activating c-Src in several human breast cancer cell lines. *J. Biol. Chem.* 275:41439–41446. <http://dx.doi.org/10.1074/jbc.M004852200>
- Bunch, T.A., Y. Grinblat, and L.S. Goldstein. 1988. Characterization and use of the *Drosophila* metallothionein promoter in cultured *Drosophila melanogaster* cells. *Nucleic Acids Res.* 16:1043–1061. <http://dx.doi.org/10.1093/nar/16.3.1043>
- Caraux, A., B. Klein, B. Paiva, C. Bret, A. Schmitz, G.M. Fuhler, N.A. Bos, H.E. Johnsen, A. Orfao, and M. Perez-Andres; Myeloma Stem Cell Network. 2010. Circulating human B and plasma cells. Age-associated changes in counts and detailed characterization of circulating normal CD138⁺ and CD138⁺ plasma cells. *Haematologica.* 95:1016–1020. <http://dx.doi.org/10.3324/haematol.2009.018689>
- Catalán, D., O. Aravena, F. Sabugo, P. Wurmman, L. Soto, A.M. Kalergis, M. Cuchacovich, and J.C. Aguilón; Millenium Nucleus on Immunology and Immunotherapy P-07-088-F 2010. B cells from rheumatoid arthritis patients show important alterations in the expression of CD86 and FcγRIIb, which are modulated by anti-tumor necrosis factor therapy. *Arthritis Res. Ther.* 12:R68. <http://dx.doi.org/10.1186/ar2985>
- Christensen, S.R., M. Kashgarian, L. Alexopoulou, R.A. Flavell, S. Akira, and M.J. Shlomchik. 2005. Toll-like receptor 9 controls anti-DNA autoantibody production in murine lupus. *J. Exp. Med.* 202:321–331. <http://dx.doi.org/10.1084/jem.20050338>
- Cicirelli, M.F., N.K. Tonks, C.D. Diltz, J.E. Weiel, E.H. Fischer, and E.G. Krebs. 1990. Microinjection of a protein-tyrosine-phosphatase inhibits insulin action in *Xenopus* oocytes. *Proc. Natl. Acad. Sci. USA.* 87:5514–5518. <http://dx.doi.org/10.1073/pnas.87.14.5514>
- Craxton, A., G. Shu, J.D. Graves, J. Saklatvala, E.G. Krebs, and E.A. Clark. 1998. p38 MAPK is required for CD40-induced gene expression and proliferation in B lymphocytes. *J. Immunol.* 161:3225–3236.
- Cuadrado, A., and A.R. Nebreda. 2010. Mechanisms and functions of p38 MAPK signalling. *Biochem. J.* 429:403–417. <http://dx.doi.org/10.1042/BJ20100323>
- Davidson, W.F., H.C. Morse III, S.O. Sharrow, and T.M. Chused. 1979. Phenotypic and functional effects of the motheaten gene on murine B and T lymphocytes. *J. Immunol.* 122:884–891.
- Dubé, N., A. Bourdeau, K.M. Heinonen, A. Cheng, A.L. Loy, and M.L. Tremblay. 2005. Genetic ablation of protein tyrosine phosphatase 1B accelerates lymphomagenesis of p53-null mice through the regulation of B-cell development. *Cancer Res.* 65:10088–10095. <http://dx.doi.org/10.1158/0008-5472.CAN-05-1353>
- Elchebly, M., P. Payette, E. Michaliszyn, W. Cromlish, S. Collins, A.L. Loy, D. Normandin, A. Cheng, J. Himms-Hagen, C.C. Chan, et al. 1999. Increased insulin sensitivity and obesity resistance in mice lacking the protein tyrosine phosphatase-1B gene. *Science.* 283:1544–1548. <http://dx.doi.org/10.1126/science.283.5407.1544>
- Elgueta, R., M.J. Benson, V.C. de Vries, A. Wasiuk, Y. Guo, and R.J. Noelle. 2009. Molecular mechanism and function of CD40/CD40L engagement in the immune system. *Immunol. Rev.* 229:152–172. <http://dx.doi.org/10.1111/j.1600-065X.2009.00782.x>
- Engel, P., J.A. Gómez-Puerta, M. Ramos-Casals, F. Lozano, and X. Bosch. 2011. Therapeutic targeting of B cells for rheumatic autoimmune diseases. *Pharmacol. Rev.* 63:127–156. <http://dx.doi.org/10.1124/pr.109.002006>
- Flint, A.J., T. Tiganis, D. Barford, and N.K. Tonks. 1997. Development of “substrate-trapping” mutants to identify physiological substrates of protein tyrosine phosphatases. *Proc. Natl. Acad. Sci. USA.* 94:1680–1685. <http://dx.doi.org/10.1073/pnas.94.5.1680>
- Frangioni, J.V., P.H. Beahm, V. Shifrin, C.A. Jost, and B.G. Neel. 1992. The nontransmembrane tyrosine phosphatase PTP-1B localizes to the endoplasmic reticulum via its 35 amino acid C-terminal sequence. *Cell.* 68:545–560. [http://dx.doi.org/10.1016/0092-8674\(92\)90190-N](http://dx.doi.org/10.1016/0092-8674(92)90190-N)
- Frangioni, J.V., A. Oda, M. Smith, E.W. Salzman, and B.G. Neel. 1993. Calpain-catalyzed cleavage and subcellular relocation of protein phosphotyrosine phosphatase 1B (PTP-1B) in human platelets. *EMBO J.* 12:4843–4856.
- Fukada, T., and N.K. Tonks. 2001. The reciprocal role of Egr-1 and Sp family proteins in regulation of the PTP1B promoter in response to the p21 Bcr-Abl oncoprotein-tyrosine kinase. *J. Biol. Chem.* 276:25512–25519. <http://dx.doi.org/10.1074/jbc.M101354200>
- Gross, J.A., S.R. Dillon, S. Mudri, J. Johnston, A. Littau, R. Roque, M. Rixon, O. Schou, K.P. Foley, H. Haugen, et al. 2001. TAC1-Ig

- neutralizes molecules critical for B cell development and autoimmune disease. Impaired B cell maturation in mice lacking BlyS. *Immunity*. 15:289–302. [http://dx.doi.org/10.1016/S1074-7613\(01\)00183-2](http://dx.doi.org/10.1016/S1074-7613(01)00183-2)
- Heinonen, K.M., N. Dubé, A. Bourdeau, W.S. Lapp, and M.L. Tremblay. 2006. Protein tyrosine phosphatase 1B negatively regulates macrophage development through CSF-1 signaling. *Proc. Natl. Acad. Sci. USA*. 103:2776–2781. <http://dx.doi.org/10.1073/pnas.0508563103>
- Hobeika, E., S. Thiemann, B. Storch, H. Jumaa, P.J. Nielsen, R. Pelanda, and M. Reth. 2006. Testing gene function early in the B cell lineage in mb1-cre mice. *Proc. Natl. Acad. Sci. USA*. 103:13789–13794. <http://dx.doi.org/10.1073/pnas.0605944103>
- Julien, S.G., N. Dubé, M. Read, J. Penney, M. Paquet, Y. Han, B.P. Kennedy, W.J. Muller, and M.L. Tremblay. 2007. Protein tyrosine phosphatase 1B deficiency or inhibition delays ErbB2-induced mammary tumorigenesis and protects from lung metastasis. *Nat. Genet.* 39:338–346. <http://dx.doi.org/10.1038/ng1963>
- Kurosaki, T., and M. Hikida. 2009. Tyrosine kinases and their substrates in B lymphocytes. *Immunol. Rev.* 228:132–148. <http://dx.doi.org/10.1111/j.1600-065X.2008.00748.x>
- Lammers, R., B. Bossenmaier, D.E. Cool, N.K. Tonks, J. Schlessinger, E.H. Fischer, and A. Ullrich. 1993. Differential activities of protein tyrosine phosphatases in intact cells. *J. Biol. Chem.* 268:22456–22462.
- LaMontagne, K.R. Jr., A.J. Flint, B.R. Franza Jr., A.M. Pandergast, and N.K. Tonks. 1998. Protein tyrosine phosphatase 1B antagonizes signalling by oncoprotein tyrosine kinase p210 bcr-abl in vivo. *Mol. Cell. Biol.* 18:2965–2975.
- Lau, C.M., C. Broughton, A.S. Tabor, S. Akira, R.A. Flavell, M.J. Mamula, S.R. Christensen, M.J. Shlomchik, G.A. Viglianti, I.R. Rifkin, and A. Marshak-Rothstein. 2005. RNA-associated autoantigens activate B cells by combined B cell antigen receptor/Toll-like receptor 7 engagement. *J. Exp. Med.* 202:1171–1177. <http://dx.doi.org/10.1084/jem.20050630>
- Lin, Q., J.R. Gu, T.W. Li, F.C. Zhang, Z.M. Lin, Z.T. Liao, Q.J. Wei, S.Y. Cao, and L. Li. 2009. Value of the peripheral blood B-cells subsets in patients with ankylosing spondylitis. *Chin. Med. J. (Engl.)*. 122:1784–1789.
- Liu, G. 2004. Technology evaluation: ISIS-113715, Isis. *Curr. Opin. Mol. Ther.* 6:331–336.
- Lu, X., R. Malumbres, B. Shields, X. Jiang, K.A. Sarosiek, Y. Natkunam, T. Tiganis, and I.S. Lossos. 2008. PTP1B is a negative regulator of interleukin 4-induced STAT6 signaling. *Blood*. 112:4098–4108. <http://dx.doi.org/10.1182/blood-2008-03-148726>
- Mackay, F., S.A. Woodcock, P. Lawton, C. Ambrose, M. Baetscher, P. Schneider, J. Tschopp, and J.L. Browning. 1999. Mice transgenic for BAFF develop lymphocytic disorders along with autoimmune manifestations. *J. Exp. Med.* 190:1697–1710. <http://dx.doi.org/10.1084/jem.190.11.1697>
- Matsushita, T., M. Fujimoto, M. Hasegawa, Y. Matsushita, K. Komura, F. Ogawa, R. Watanabe, K. Takehara, and S. Sato. 2007. BAFF antagonist attenuates the development of skin fibrosis in tight-skin mice. *J. Invest. Dermatol.* 127:2772–2780.
- Mecklenbräuker, I., S.L. Kalled, M. Leitges, F. Mackay, and A. Tarakhovskiy. 2004. Regulation of B-cell survival by BAFF-dependent PKC δ -mediated nuclear signalling. *Nature*. 431:456–461. <http://dx.doi.org/10.1038/nature02955>
- Mei, H.E., D. Frölich, C. Giesecke, C. Lodenkemper, K. Reiter, S. Schmidt, E. Feist, C. Daridon, H.-P. Tony, A. Radbruch, and T. Dörner. 2010. Steady-state generation of mucosal IgA⁺ plasmablasts is not abrogated by B-cell depletion therapy with rituximab. *Blood*. 116:5181–5190. <http://dx.doi.org/10.1182/blood-2010-01-266536>
- Myers, M.P., J.N. Andersen, A. Cheng, M.L. Tremblay, C.M. Horvath, J.P. Parisien, A. Salmeen, D. Barford, and N.K. Tonks. 2001. TYK2 and JAK2 are substrates of protein-tyrosine phosphatase 1B. *J. Biol. Chem.* 276:47771–47774.
- Pao, L.L., K. Badour, K.A. Siminovitch, and B.G. Neel. 2007a. Nonreceptor protein-tyrosine phosphatases in immune cell signaling. *Annu. Rev. Immunol.* 25:473–523. <http://dx.doi.org/10.1146/annurev.immunol.25.021704.115647>
- Pao, L.L., K.-P. Lam, J.M. Henderson, J.L. Kutok, M. Alimzhanov, L. Nitschke, M.L. Thomas, B.G. Neel, and K. Rajewsky. 2007b. B cell-specific deletion of protein-tyrosine phosphatase Shp1 promotes B-1a cell development and causes systemic autoimmunity. *Immunity*. 27:35–48. <http://dx.doi.org/10.1016/j.immuni.2007.04.016>
- Raingaud, J., A.J. Whitmarsh, T. Barrett, B. Dérjard, and R.J. Davis. 1996. MKK3- and MKK6-regulated gene expression is mediated by the p38 mitogen-activated protein kinase signal transduction pathway. *Mol. Cell. Biol.* 16:1247–1255.
- Rolli, V., M. Gallwitz, T. Wossning, A. Flemming, W.W. Schamel, C. Zürn, and M. Reth. 2002. Amplification of B cell antigen receptor signaling by a Syk/ITAM positive feedback loop. *Mol. Cell.* 10:1057–1069. [http://dx.doi.org/10.1016/S1097-2765\(02\)00739-6](http://dx.doi.org/10.1016/S1097-2765(02)00739-6)
- Sack, U., K. Conrad, E. Csernok, I. Frank, F. Hiepe, T. Krieger, A. Kromminga, P. von Landenberg, G. Messer, T. Witte, and R. Mierau; German EASI (European Autoimmunity Standardization Initiative). 2009. Autoantibody detection using indirect immunofluorescence on HEP-2 cells. *Ann. N. Y. Acad. Sci.* 1173:166–173. <http://dx.doi.org/10.1111/j.1749-6632.2009.04735.x>
- Schiemann, B., J.L. Gommerman, K. Vora, T.G. Cachero, S. Shulga-Morskaya, M. Dobles, E. Frew, and M.L. Scott. 2001. An essential role for BAFF in the normal development of B cells through a BCMA-independent pathway. *Science*. 293:2111–2114. <http://dx.doi.org/10.1126/science.1061964>
- Seyfert, V.L., S. McMahon, W. Glenn, X.M. Cao, V.P. Sukhatme, and J.G. Monroe. 1990. Egr-1 expression in surface Ig-mediated B cell activation. Kinetics and association with protein kinase C activation. *J. Immunol.* 145:3647–3653.
- Shrestha, S., B.R. Bhattarai, H. Cho, J.K. Choi, and H. Cho. 2007. PTP1B inhibitor Ertiprotafib is also a potent inhibitor of I κ B kinase β (IKK- β). *Bioorg. Med. Chem. Lett.* 17:2728–2730. <http://dx.doi.org/10.1016/j.bmcl.2007.03.001>
- Shultz, L.D., and M.C. Green. 1976. Motheaten, an immunodeficient mutant of the mouse. II. Depressed immune competence and elevated serum immunoglobulins. *J. Immunol.* 116:936–943.
- Szysko, E.A., J.G. Brun, K. Skarstein, A.B. Peck, R. Jonsson, and K.A. Brokstad. 2011. Phenotypic diversity of peripheral blood plasma cells in primary Sjögren's syndrome. *Scand. J. Immunol.* 73:18–28. <http://dx.doi.org/10.1111/j.1365-3083.2010.02475.x>
- Vang, T., A.V. Miletic, Y. Arimura, L. Tautz, R.C. Rickert, and T. Mustelin. 2008. Protein tyrosine phosphatases in autoimmunity. *Annu. Rev. Immunol.* 26:29–55. <http://dx.doi.org/10.1146/annurev.immunol.26.021607.090418>
- Viglianti, G.A., C.M. Lau, T.M. Hanley, B.A. Miko, M.J. Shlomchik, and A. Marshak-Rothstein. 2003. Activation of autoreactive B cells by CpG dsDNA. *Immunity*. 19:837–847. [http://dx.doi.org/10.1016/S1074-7613\(03\)00323-6](http://dx.doi.org/10.1016/S1074-7613(03)00323-6)
- Xie, L., S.-Y. Lee, J.N. Andersen, S. Waters, K. Shen, X.-L. Guo, N.P.H. Moller, J.M. Olefsky, D.S. Lawrence, and Z.-Y. Zhang. 2003. Cellular effects of small molecule PTP1B inhibitors on insulin signaling. *Biochemistry*. 42:12792–12804. <http://dx.doi.org/10.1021/bi035238p>
- Xu, H., H. An, J. Hou, C. Han, P. Wang, Y. Yu, and X. Cao. 2008. Phosphatase PTP1B negatively regulates MyD88- and TRIF-dependent proinflammatory cytokine and type I interferon production in TLR-triggered macrophages. *Mol. Immunol.* 45:3545–3552. <http://dx.doi.org/10.1016/j.molimm.2008.05.006>
- Yanaba, K., J.D. Bouaziz, T. Matsushita, C.M. Magro, E.W. St Clair, and T.F. Tedder. 2008. B-lymphocyte contributions to human autoimmune disease. *Immunol. Rev.* 223:284–299. <http://dx.doi.org/10.1111/j.1600-065X.2008.00646.x>
- Zheng, Y., S. Gallucci, J.P. Gaughan, J.A. Gross, and M. Monestier. 2005. A role for B cell-activating factor of the TNF family in chemically induced autoimmunity. *J. Immunol.* 175:6163–6168.